Protein Structures

DOI: 10.1002/anie.201004422

Conformation of a Seven-Helical Transmembrane Photosensor in the Lipid Environment**

Lichi Shi, Izuru Kawamura, Kwang-Hwan Jung, Leonid S. Brown, and Vladimir Ladizhansky**

Solid-state NMR spectroscopy (SSNMR) has emerged as one of the main tools for structural and dynamic investigation of membrane proteins in their native-like lipid environment, and has already provided a wealth of information on a number of biologically and medically important systems.[1–8] Applications to large helical proteins are underway and promise to add to our understanding of membrane biology.[9–13]

Herein we present a magic-angle spinning[14] (MAS) SSNMR study of a seven-helical membrane photoreceptor, sensory rhodopsin from *Anabaena* sp. PCC 7120 (ASR).[15] We report the assignment of backbone and side-chain signals of the protein, analysis of its secondary structure, and analysis of the environment of many polar residues. We use site-specific H/D exchange measurements to determine the water-accessible surface of the protein and its topology within the lipid bilayer. Although the secondary structure of ASR derived from our data is overall consistent with that previously determined by X-ray crystallography,[16] we have identified a number of important differences and additions, which allowed us to build a refined structural model.

We employed 3D chemical shift correlation spectroscopy performed on a single lipid-reconstituted uniformly ^{13}C,^{15}N-labeled sample. From a structural perspective, ASR shares its seven-helical architecture with G-protein-coupled receptors. Our studies demonstrate that a similar methodology can in principle be applied to this class of proteins without the need for crystallization and/or detergent solubilization. Importantly, the structural information obtained from SSNMR pertains to a protein in the lipid environment, closely related to its native state. ASR reconstituted in lipids gives well-resolved spectra with high signal-to-noise ratios, with typical carbon and nitrogen line widths of 0.5 ppm (Figure 1 and Figure S1 in the Supporting Information). The protein is functional and stable in this environment.[17]

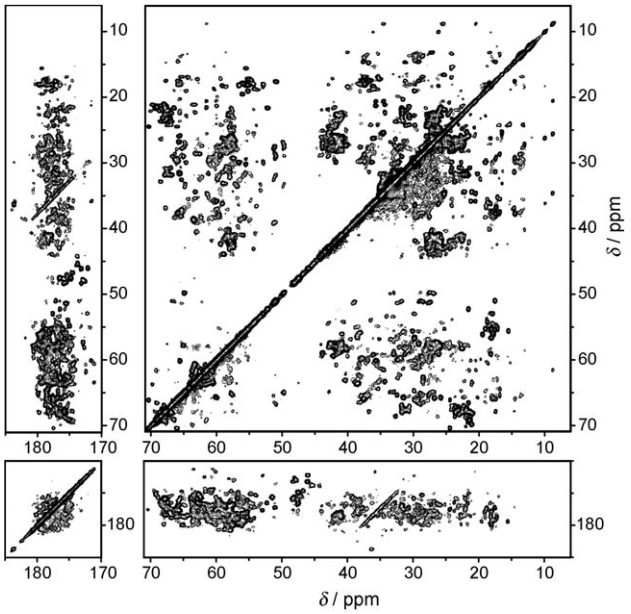

Figure 1. 2D DARR ^{13}C–^{13}C correlation spectrum of ASR recorded at a proton frequency of 800 MHz.

Spectroscopic assignments were obtained from five 3D chemical shift correlation experiments acquired on a single sample: CONCA, two NCACX experiments with dipole-assisted rotamer resonance (DARR)[18] mixing times of 20 ms and 50 ms, and two NCOCX experiments with DARR mixing times of 50 ms and 100 ms. While the CONCA spectrum provides nearly complete backbone resolution and establishes inter-residue correlations between CO[*i*], N[*i*+1], and CA-[*i*+1] atoms, the NCACX and NCOCX experiments allow to record chemical shifts of the side-chain carbon atoms for identification of the amino acid type. Shorter mixing time experiments provide mostly one- and two-bond correlations, for example, N[*i*+1]–CO[*i*]–CA[*i*] and N[*i*]–CA[*i*]–CO[*i*]/CB[*i*] in NCOCX and NCACX experiments, while longer mixing times establish shifts of the entire carbon side chain, and provide additional inter-residue correlations for assignment validation.

The three types of spectra can be coanalyzed to construct a sequential backbone walk (Figure 2 and Figure S2). Back-

[*] Dr. L. Shi,[+] Dr. L. S. Brown, Dr. V. Ladizhansky
Department of Physics, University of Guelph
50 Stone Rd. E., Guelph, Ontario, N1G 2W1 (Canada)
Fax: (+1) 519-836-9967
E-mail: lebrown@uoguelph.ca
vladizha@uoguelph.ca
Dr. I. Kawamura[+]
Faculty of Engineering, Yokohama National University
79-5 Tokiwadai, Hodogaya-ku, Yokohama 240-8501 (Japan)
Dr. K.-H. Jung
Department of Life Science, Sogang University
Shinsu-Dong, Mapo-Gu, Seoul (Korea)
[+] These authors contributed equally to this work.

[**] This research was supported by the Natural Science Engineering Research Council of Canada, the Canada Foundation for Innovation, the Ontario Ministry of Research and Innovation, and the National Research Foundation of Korea (2008-0060997). V.L. holds the Canada Research Chair in Biophysics. We thank Dr. Steffen P. Graether for proofreading the manuscript.

Supporting information for this article is available on the WWW under http://dx.doi.org/10.1002/anie.201004422.

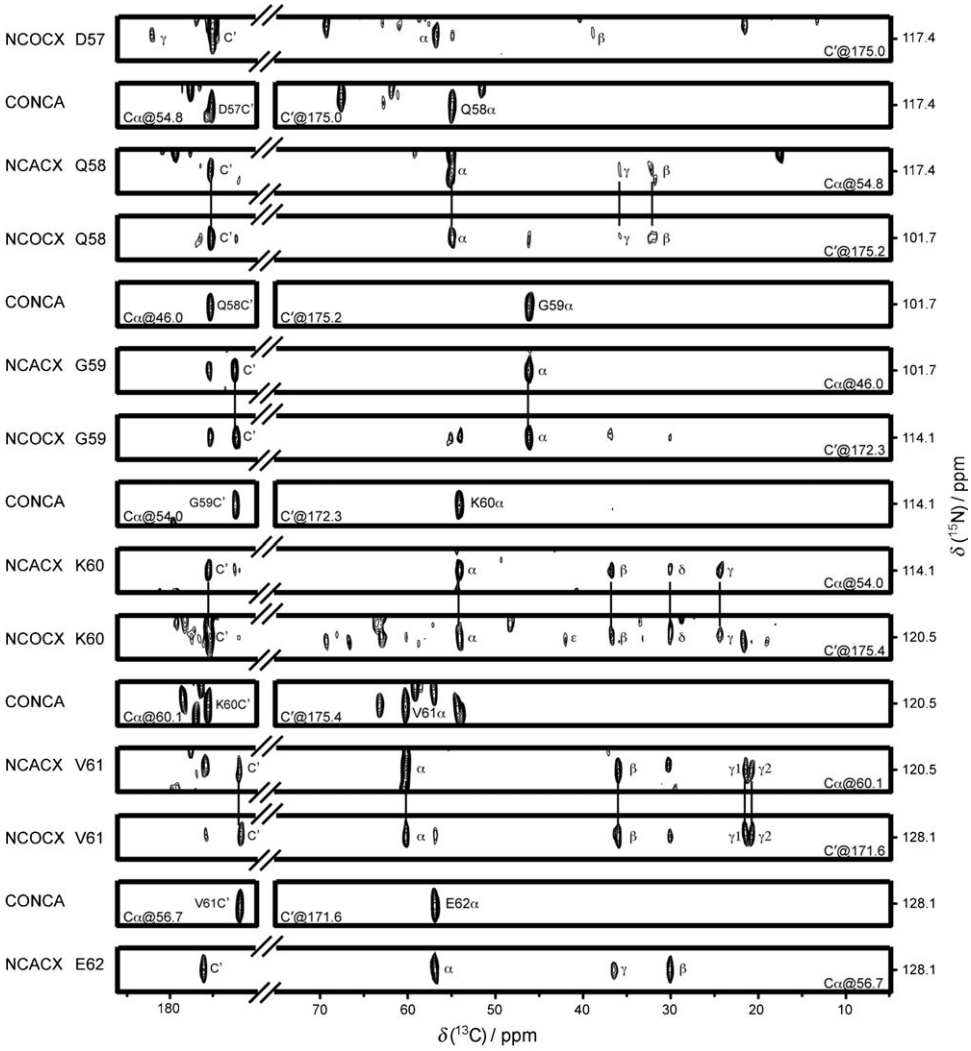

Figure 2. An example of a sequential assignment walk for the D57–E62 fragment of ASR, which is a part of the B–C loop that is missing in the X-ray structure.

bone and side-chain resonances for approximately 85 % of the transmembrane (TM) region and for many residues in the loop regions have been assigned (see the Supporting Information). An additional 46 spin systems were identified but could not be assigned. Thus, we could detect the majority of residues (ca. 91 %), including those in the loops and tails, similar to our results in proteorhodopsin,[13] which has loops and tails of similar length. In contrast, extra-membranous parts of sensory rhodopsin II (SR-II) appear to be more mobile.[10]

The secondary structure of the protein derived from the C^{α} and C^{β} secondary chemical shifts[19] is shown in Figure 3. There are seven largely uninterrupted positive stretches indicating the presence of seven helices. Most of the helices and their distortions are in agreement with the X-ray structure. We detected a small distortion in the helix A at M15, and at S47 in the helix B, a proline kink at V78 in helix C, as well as a large distortion at the position of retinal-flanking W76. There is a π-bulge at the Schiff base formed by K210 in helix G. Both the proline kink in helix C and the non-proline kink in helix G appear to be common structural features of microbial rhodopsins.[13,20]

There are a number of notable differences from the X-ray data. Firstly, there are two short β strands in the B–C loop, which appears to be disordered and undetectable in the X-ray data. A similar β hairpin structure was observed in several other microbial rhodopsins.[13,20,21] Secondly, SSNMR shows a different conformation of helix G, which contains a unique P206 instead of the superconserved aspartic acid. In 3D crystals of ASR, P206 induces a 3-residue helicity break in the extracellular half (residues 201–203 in the 1XIO model). On the contrary, this helix remains uninterrupted in the lipid environment. Closer examination of the dihedral angles derived from the X-ray data and from TALOS analysis[22] of chemical shifts reveals additional deviations at the extracellular ends of helices B, C, D, and F, and at the cytoplasmic end of helix F (Figure S3). Finally, from the 3D NMR data and from the 1D ^{15}N NMR spectrum (Figure S1) we identify single conformations of retinal (consis-

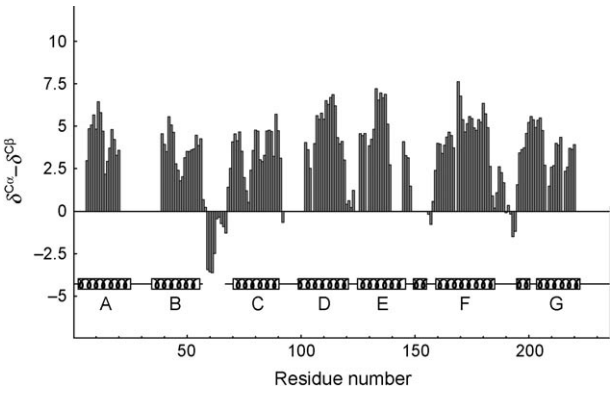

Figure 3. Secondary chemical shift difference $\delta_{C\alpha}-\delta_{C\beta}$ plotted as a function of residue number that has been averaged in a 3 residue sliding window. The secondary structure derived from the X-ray data (PDB 1XIO)[16] is shown at the bottom.

tent with retinal extraction data[23]) and of residues K210 and S86, for which X-ray crystallography gave alternate conformations.[16] We could also deduce protonation states and hydrogen-bonding strength for a number of polar side chains, including some functionally important residues (see the Supporting Information for a discussion).

To probe the water-accessible surface of the protein and identify the hydrophilic cavities in its TM portion, the sample was incubated for 24 h in a D_2O-based buffer to exchange solvent-exposed amide sites. A comparison of 2D NCA spectra of samples incubated in H_2O and D_2O recorded with short H/N cross polarization (CP) times of 300 μs reveals that peaks from many residues disappear after incubation in D_2O (Figure 4a,b). In these experiments, spins of nitrogen atoms are excited primarily from directly bonded amide protons, as evident, for example, from disappearance of all proline correlations. Thus, the signals of solvent-exposed residues are strongly attenuated.

Most of the TM residues are well-protected by tight interhelical packing, protein–lipid interactions, and by strong hydrogen bonding within the α helices, and are unaffected by the exchange. Notable exceptions are I110, K167, T170, and S209, which are completely exchanged, as well as a cytoplasmic part of helix F, which shows stretches of partial exchange (Figure 4c and Figure 5). These results imply a dynamic nature of the cytoplasmic end of helix F, which is known to tilt out in the photocycles of other microbial rhodopsins. It should be noted that residue S209 precedes the retinal-binding K210, and may be exposed to water, in consistency with the presence of a cytoplasmic hydrogen-bonded network.[13]

Most other affected residues are located on the extracellular or cytoplasmic surfaces of the protein. The signals from the entire B–C loop (D57-Y70), from many residues in the E–F loop, and at the ends of helices are eliminated by the exchange. On the other hand, G189, G191, and W192 in the F–G loop exchange only weakly, consistent with a strong hydrogen-bonding pattern predicted by the X-ray data. Overall, the exchange pattern strongly suggests that ASR is located asymmetrically in the lipid bilayer, with the cytoplasmic part being more exposed to the solvent.

To build a refined 3D model of lipid-embedded ASR, we have measured a 2D ^{13}C–^{13}C NMR correlation spectrum with a spin-diffusion mixing time of 500 ms,[1,24] which led to 9072 long-range C–C distance restraints. Among these, 703 medium- to long-range unambiguous inter-residue cross-peaks consistent with the X-ray structure were identified, and used for structure calculations[25] along with the TALOS[22] torsional restraints. To constrain unassigned protein fragments, we also included 250 interatomic distances derived from the X-ray data (see the Supporting Information for details). The resulting model, which shows water-exposed fragments and an approximate positioning of the protein in the lipid bilayer derived from H/D exchange and features the β-structured B–C loop and uninterrupted helix G, is presented in Figure 5.

In conclusion, we have shown that characterization of a heptahelical membrane protein in the lipid environment by SSNMR can reveal structural features either non-detectable or distorted in 3D crystals. The total experimental time required to collect the data was on the order of 15 days, thus demonstrating clear feasibility of rapid SSNMR structural characterization of proteins of similar fold and size. Further improvements in the NMR hardware and methodology will likely permit an extension to even larger systems.

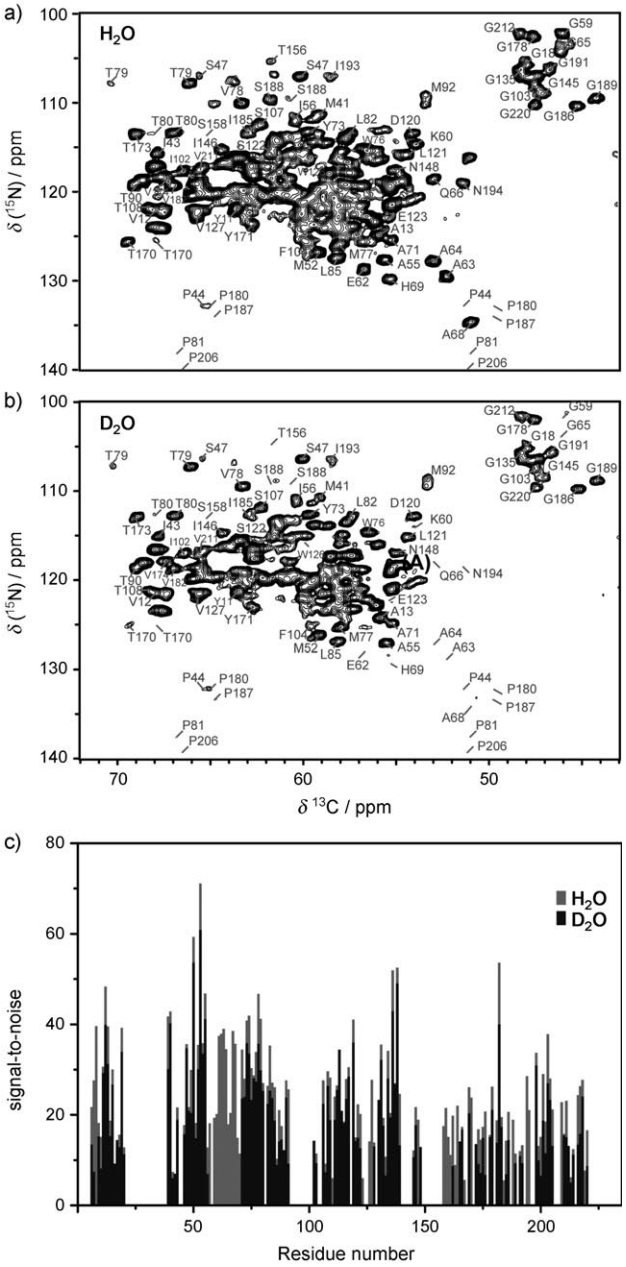

Figure 4. H/D exchange experiments. 2D NCA correlation planes measured in samples in a) H_2O-based buffer and b) after 1 day of incubation in D_2O. c) Site-specific comparison of cross-peak intensities recorded in the 3D NCACX experiment in the two samples.

Experimental Section

[U-^{13}C,^{15}N] labeled C-terminally truncated histidine-tagged ASR was expressed in BL21 RIL *E. coli* grown on M9 minimal medium at 30 °C, using U-^{13}C-glucose (4 g) and $^{15}NH_4Cl$ (1 g) per litre as the carbon and nitrogen sources. 7.5 μM retinal was added exogenously at

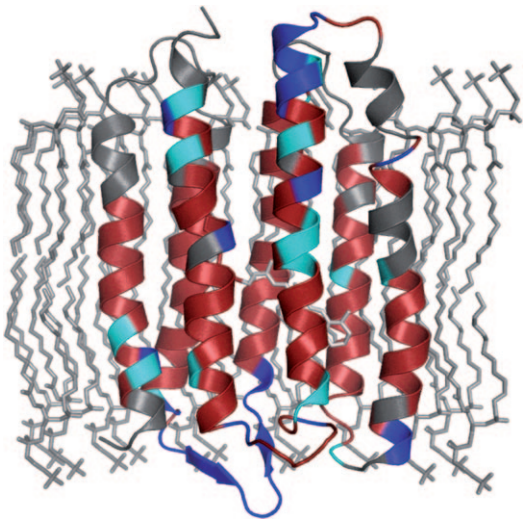

Figure 5. Structural model of ASR derived from SSNMR and X-ray data. Red: non-exchangeable residues, cyan and blue: weakly and strongly exchangeable residues, respectively. The cytoplasmic side is on top.

the time of induction to regenerate the expressed opsin. The membrane fraction was solubilized in 1% DDM (*n*-dodecyl β-D-maltoside) at 4°C. Approximately 5 mg of ASR was purified from one litre of culture. Liposomes were prepared by hydrating dried DMPC (1,2-dimyristoyl-*sn*-glycero-3-phosphocholine) and DMPA (1,2-dimyristoyl-*sn*-glycero-3-phosphate) as described previously,[13] and mixed with purified solubilized ASR, at a lipid/protein ratio of 1:2 (w/w). The functionality of the protein was tested by using visible and FTIR spectroscopy.[17]

All SSNMR experiments were performed on a Bruker Avance III spectrometer operating at 800.23 MHz, equipped with a 3.2 mm E-free ^{1}H-^{13}C-^{15}N probe. The MAS frequency was 14.3 kHz and the temperature was maintained at 5°C for all experiments. NCOCX, NCACX, and CONCA 3D experiments were performed using previously described pulse sequences, but without J-decoupling.[13,26] Further details of data acquisition and processing are given in the Supporting Information.

Received: July 19, 2010
Revised: November 8, 2010
Published online: December 29, 2010

Keywords: membrane proteins · protein structures · receptors · rhodopsin · solid-state NMR spectroscopy

[1] F. Castellani, B. van Rossum, A. Diehl, M. Schubert, K. Rehbein, H. Oschkinat, *Nature* **2002**, *420*, 98.
[2] S. H. Park, A. A. Mrse, A. A. Nevzorov, M. F. Mesleh, M. Oblatt-Montal, M. Montal, S. J. Opella, *J. Mol. Biol.* **2003**, *333*, 409.
[3] S. Sharpe, W. M. Yau, R. Tycko, *Biochemistry* **2006**, *45*, 918.
[4] S. Ahuja, V. Hornak, E. C. Yan, N. Syrett, J. A. Goncalves, A. Hirshfeld, M. Ziliox, T. P. Sakmar, M. Sheves, P. J. Reeves, S. O. Smith, M. Eilers, *Nat. Struct. Mol. Biol.* **2009**, *16*, 168.
[5] V. S. Bajaj, M. L. Mak-Jurkauskas, M. Belenky, J. Herzfeld, R. G. Griffin, *Proc. Natl. Acad. Sci. USA* **2009**, *106*, 9244.
[6] M. Yi, T. A. Cross, H. X. Zhou, *Proc. Natl. Acad. Sci. USA* **2009**, *106*, 13311.
[7] W. Qiang, Y. Sun, D. P. Weliky, *Proc. Natl. Acad. Sci. USA* **2009**, *106*, 15314.
[8] S. D. Cady, K. Schmidt-Rohr, J. Wang, C. S. Soto, W. F. Degrado, M. Hong, *Nature* **2010**, *463*, 689.
[9] A. Lange, K. Giller, S. Hornig, M. F. Martin-Eauclaire, O. Pongs, S. Becker, M. Baldus, *Nature* **2006**, *440*, 959.
[10] M. Etzkorn, S. Martell, O. C. Andronesi, K. Seidel, M. Engelhard, M. Baldus, *Angew. Chem.* **2007**, *119*, 463; *Angew. Chem. Int. Ed.* **2007**, *46*, 459.
[11] Y. Li, D. A. Berthold, R. B. Gennis, C. M. Rienstra, *Protein Sci.* **2008**, *17*, 199.
[12] J. Xu, U. H. Dürr, S. C. Im, Z. Gan, L. Waskell, A. Ramamoorthy, *Angew. Chem.* **2008**, *120*, 7982; *Angew. Chem. Int. Ed.* **2008**, *47*, 7864.
[13] L. Shi, M. A. M. Ahmed, W. Zhang, G. Whited, L. S. Brown, V. Ladizhansky, *J. Mol. Biol.* **2009**, *386*, 1078.
[14] E. R. Andrew, A. Bradbury, R. G. Eades, *Nature* **1958**, *182*, 1659.
[15] K. H. Jung, V. D. Trivedi, J. L. Spudich, *Mol. Microbiol.* **2003**, *47*, 1513.
[16] L. Vogeley, O. A. Sineshchekov, V. D. Trivedi, J. Sasaki, J. L. Spudich, H. Luecke, *Science* **2004**, *306*, 1390.
[17] L. C. Shi, S. R. Yoon, A. G. Bezerra, K. H. Jung, L. S. Brown, *J. Mol. Biol.* **2006**, *358*, 686.
[18] K. Takegoshi, S. Nakamura, T. Terao, *Chem. Phys. Lett.* **2001**, *344*, 631.
[19] D. S. Wishart, B. D. Sykes, F. M. Richards, *Biochemistry* **1992**, *31*, 1647.
[20] H. Luecke, B. Schobert, H. T. Richter, J. P. Cartailler, J. K. Lanyi, *J. Mol. Biol.* **1999**, *291*, 899.
[21] H. Luecke, B. Schobert, J. Stagno, E. S. Imasheva, J. M. Wang, S. P. Balashov, J. K. Lanyi, *Proc. Natl. Acad. Sci. USA* **2008**, *105*, 16561.
[22] G. Cornilescu, F. Delaglio, A. Bax, *J. Biomol. NMR* **1999**, *13*, 289.
[23] A. Kawanabe, Y. Furutani, S. R. Yoon, K. H. Jung, H. Kandori, *Biochemistry* **2008**, *47*, 10033.
[24] T. Manolikas, T. Herrmann, B. H. Meier, *J. Am. Chem. Soc.* **2008**, *130*, 3959.
[25] A. T. Brünger, P. D. Adams, G. M. Clore, W. L. DeLano, P. Gros, R. W. Grosse-Kunstleve, J. S. Jiang, J. Kuszewski, M. Nilges, N. S. Pannu, R. J. Read, L. M. Rice, T. Simonson, G. L. Warren, *Acta Crystallogr. Sect. D* **1998**, *54*, 905.
[26] L. Shi, E. M. Lake, M. A. Ahmed, L. S. Brown, V. Ladizhansky, *Biochim. Biophys. Acta Biomembr.* **2009**, *1788*, 2563.

